Journal Name

ARTICLE

Subunit-subunit interactions play a key role in the heme-degradation reaction of HutZ from *Vibrio cholerae*

Received 00th January 20xx,
Accepted 00th January 20xx

DOI: 10.1039/x0xx00000x

www.rsc.org/

Takeshi Uchida,*[a,b] Kazuki Ohta,[b] Yukari Sekine,[b] Nobuhiko Dojun,[b] and Koichiro Ishimori[a,b]

HutZ, a dimeric protein, from *Vibrio cholerae* is a protein that catalyzes the oxygen-dependent degradation of heme. Interestingly, the ascorbic acid-supported heme-degradation activity of HutZ depends on pH: less than 10% of heme is degraded by HutZ at pH 8.0, but nearly 90% of heme is degraded at pH 6.0. We examined here pH-dependent conformational changes in HutZ using fluorescence spectroscopy. Trp109 is estimated to be located approximately 21 Å from heme and is present in a different subunit containing a heme axial ligand. Thus, we postulated that the distance between heme and Trp109 reflects subunit-subunit orientational changes. On the basis of resonance energy transfer from Trp109 to heme, we estimated the distance between heme and Trp109 to be approximately 17 Å at pH 8.0, while the distance increased by less than 2 Å at pH 6.0. We presumed that such changes led to a decrease in electron donation from the proximal histidine, resulting in enhancement of the heme-degradation activity. To confirm this scenario, we mutated Ala31, located at the dimer interface, to valine to alter the distance through the subunit-subunit interaction. The distance between heme and Trp109 for the A31V mutant was elongated to 24–27 Å. Although resonance Raman spectra and reduction rate of heme suggested that this mutation resulted in diminished electron donation from the heme axial ligand, ascorbic acid-supported heme-degradation activity was not observed. Based on our findings, it can be proposed that the relative positioning of two protomers is important in determining the heme degradation rate by HutZ.

1. Introduction

Almost all bacteria require iron for their survival and have developed sophisticated mechanisms for solubilizing, sequestering, and releasing iron within the cell. Most bacterial pathogens have evolved to take advantage of heme-containing host proteins as a source of iron. Thus, the ability to transport and utilize heme is a common mechanism employed by pathogenic bacteria to establish and maintain infection.[1–6]

The exogenously acquired heme is subsequently oxidized by a heme-degrading enzyme to release iron for utilization by the bacteria. Heme degradation is a metabolic function performed by diverse organisms. Extensive studies on mammalian heme oxygenase (HO) have revealed the precise mechanism of heme degradation,[7–9] demonstrating that HO binds heme as a substrate, which is reduced to the ferrous form, followed by formation of oxyferrous heme (Fe^{2+}–O_2). The oxyferrous heme is converted to ferric hydroperoxy heme (Fe^{3+}–OOH), which reacts with the heme macrocycle to give α-*meso* hydroxyheme. The hydroxylated α-*meso* carbon is then eliminated as carbon monoxide (CO) with the concomitant formation of verdoheme in the presence of O_2. Verdoheme is subsequently oxidized to biliverdin.

Bacterial HOs with high homology to mammalian HO have been discovered over the last decade.[10–14] These HOs exhibit significant structural similarity to mammalian HOs and share the same heme-degradation pathway. Recently, new members of the heme-degrading enzyme family were discovered in *Staphylococcus aureus*.[15–17] These enzymes, called IsdG and IsdI, have no sequence or structural homology with mammalian HOs. Furthermore, IsdG-family enzymes have a unique heme-degrading mechanism, in which heme is converted to staphylobilin with the release of *meso*-carbon as formaldehyde, not as CO.[18–20] Recently, an oxygen-independent heme-degrading enzyme, ChuW, was discovered in *Escherichia coli* O157:H7.[21] ChuW, *S*-adenosylmethionine methyltransferase, anaerobically catalyzes radical-mediated heme degradation.

Recent studies have reported that HugZ from *Helicobacter pylori*, possesses heme-degrading activity despite lacking sequence homology with mammalian HOs or IsdG and IsdI.[22,23] Genome sequence analyses have revealed that *Vibrio cholerae* contains a homologous protein called HutZ.[24] Previously, we found that HutZ from *V. cholerae* degrades heme to biliverdin via a verdoheme intermediate (Scheme 1),[25,26] as is the case for HO catalysis.[27–29] This finding coincided with the fact that *V. cholerae* mutant that lost the *hutZ* gene does not grow well when heme is the sole iron source.[30] The cleavage site is the β- or δ-*meso* position, not the α-*meso* position, as observed in

[a] Department of Chemistry, Faculty of Science, Hokkaido University, Sapporo 060-0810, Japan. E-mail: uchida@sci.hokudai.ac.jp
[b] Graduate School of Chemical Sciences and Engineering, Hokkaido University, Sapporo 060-8628, Japan

†Electronic Supplementary Information (ESI) available: [details of any supplementary information available should be included here]. See DOI: 10.1039/x0xx00000x

mammalian HOs.[24] One interesting feature of HutZ is the pH dependence of its heme-degradation activity: almost no iron is released by the reaction of HutZ with ascorbic acid as an electron source at pH 8.0, but approximately 90% of heme is broken upon lowering the pH to 6.0.[25,31]

Although crystal structure of the heme-bound form of HutZ has not been available, resonance Raman spectroscopy data suggested a unique nature of the structure of heme-HutZ in the heme environment.[25] A plot of Fe-CO ($\nu_{Fe\text{-}CO}$) versus C-O ($\nu_{C\text{-}O}$) stretching modes of the CO-bound form was considerably displaced from the line corresponding to proteins possessing a neutral His as an axial ligand, but fell near the line for proteins with an imidazolate-like residue as an axial ligand. Close inspection of the crystal structure of a homologous HugZ protein from *H. pylori* showed that Asp207, which is conserved in HutZ from *V. cholerae* (as Asp132), is located within range to make hydrogen bond contact with the proximal His (Fig. S1†).[22] Such proximal His-Asp hydrogen bonding is known to impose an imidazolate character on the axial His, as observed in most peroxidases.[32–34] The proximal hydrogen bond that is typically present in heme peroxidases is favorable for activation of O_2, but not for heme degradation,[35] because it promotes cleavage of the O-O bond of the hydroperoxy heme to produce a high-valent iron-oxo species, which has no heme-degradation activity.[36] Therefore, the presence of a strong proximal hydrogen bond in heme-HutZ seemed to be an unfavorable characteristic for a heme-degrading enzyme. To confirm this, site-directed mutagenesis of Asp132 had previously been performed to reduce electron donation from His170.[37] Unexpectedly, replacement of Asp132 with Asn or Leu was shown to result in a decrease in heme-degradation activity, whereas replacement with Glu, which preserved the proximal hydrogen bond between His170 and Glu132, had little effect on this activity. This result suggests that the hydrogen bond between His170 and Asp132 is not a predominant factor in repressing the heme-degradation activity of HutZ. The crystal structure of HugZ shows this protein to be dimer protein (Fig. 1), which is also true of HutZ as determined by size exclusion chromatography.[25] Unlike most peroxidases, the hydrogen bond partner (Asp132) of the heme axial ligand (His170) comes from another protomer. This character might be correlated to less peroxidase activity in spite of the strong hydrogen bond between Asp132 and His170 (Fig. S1†).

We further recently succeeded in obtaining the Fe-O_2 stretching mode ($\nu_{Fe\text{-}O2}$) for heme-HutZ using a rapid mixing technique combined with resonance Raman spectroscopy.[26] The frequency of $\nu_{Fe\text{-}O2}$ for oxyferrous heme-HutZ was 565 cm^{-1}—significantly lower than that for P450 and nitric oxide synthase with Cys as a heme axial ligand (~520 cm^{-1}),[38,39] but close to that for proteins with His as a heme axial ligand (~565 cm^{-1} for hemoglobin).[40,41] The fact that $\nu_{Fe\text{-}O2}$ for oxyferrous heme-HutZ was almost the same as that for HO[42] indicated that electron donation from the proximal His of HutZ was at the same level as that of HO, but not as strong as P450 or nitric oxide synthase. This result raised the question of strong electron donation from His170.

In addition to the pH dependence of the heme-degradation activity of HutZ, a pH-dependent structural change in the heme distal site has been reported.[25] The absorption spectra of heme-HutZ depended on the pH, a dependence that was derived from a spin-state transition of the heme between Fe^{3+}–H_2O (high-spin heme) and Fe^{3+}–OH^- (low-spin heme). The pK_a value of the transition was reported to be less than 7,[25] which is lower than that of most HOs.[43–46] The relationship between the spin state of the ferric heme and heme-degradation activity suggested that the conformational change in the heme distal site is transmitted to the proximal site through the subunit-subunit interaction, which is a key factor for HutZ to be active.

In this paper, we found that replacement of Ala31, which is located at the dimer interface of HutZ, with Val decreased electron donation from the proximal heme ligand, even at pH

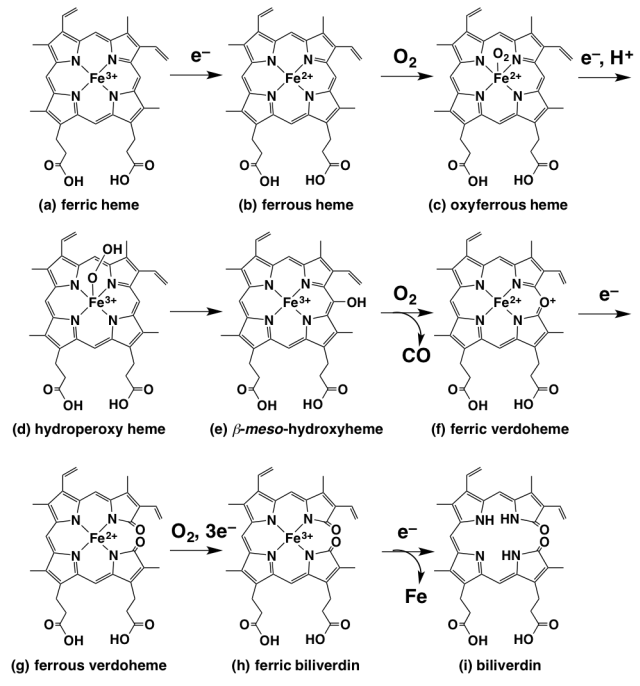

Scheme 1 Proposed heme degradation mechanism of HutZ.

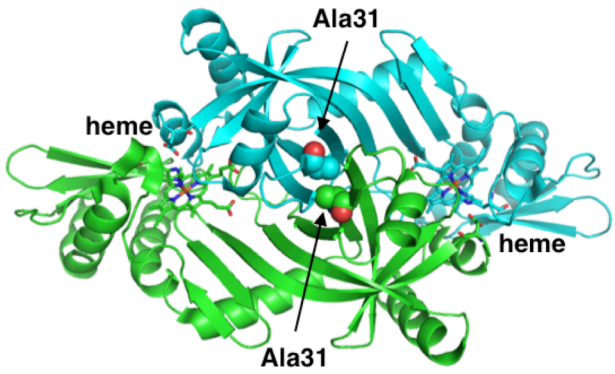

Fig. 1 Crystal structure of HugZ from *H. pylori* (Protein Data Bank entry 3GAS). Residues are numbered according to the amino acid sequence of HutZ from *V. cholerae*.

8.0, despite the fact that heme retained the low-spin state. Thus, this mutant was a good model for examining the relationship between electron donation from the heme proximal ligand and heme-degradation activity. The A31V mutant exhibited diminished electron donation, while also showing a decrease in heme-degradation activity, indicating that proximal electron donation is not the sole determinant of the reactivity of HutZ. Fluorescence spectra revealed that the introduction of a larger residue at position 31 is associated with realignment of subunit-subunit interactions. We also found that a slight change of relative orientation of protomers occurs when wild-type HutZ is converted to be active upon lowering the pH to 6.0. Consequently, a conformational change that includes interactions at the interface between two protomers appears to be essential for HutZ to degrade heme. This activation mechanism would be advantageous for *V. cholerae*, as it would allow toxic iron to be obtained only when needed.

2. Materials and methods

Materials

The chemicals used in this study were purchased from Wako Pure Chemical Industries (Osaka, Japan), Nacalai Tesque (Kyoto, Japan) or Sigma-Aldrich (St. Louis, MO, USA), and used without further purification.

Protein Expression and Purification

HutZ mutant proteins were expressed and purified as described previously.[25] Briefly, the *HutZ* gene was subcloned into pET-28b (Merck Millipore, Darmstadt, Germany) via *Nde*I and *EcoR*I sites, and the thrombin recognition site (Leu-Val-Pro-Arg-Gly-Ser) in the pET-28b construct was mutated to the HRV 3C protease recognition site (Leu-Glu-Val-Leu-Phe-Gln-Gly-Pro).[47] *E. coli* strains transduced with HutZ expression plasmids were grown at 37 °C in LB broth supplemented with 50 μg/mL kanamycin. After cells reached an optical density at 600 nm (OD_{600}) of 0.6–1.0, expression of His-tagged fusion protein in *E. coli* BL21(DE3) was induced by adding isopropyl-β-D-thiogalactopyranoside to a final concentration of 0.4 mM, after which cells were further incubated at 28 °C overnight. The cells were harvested by centrifugation and suspended in lysis buffer containing 50 mM Tris-HCl, 150 mM NaCl, and 0.1% Nonidet P-40 (pH 8.0). Cells (~5.0 g) obtained from 1 L of culture were incubated for 60 min on ice with 1 mg/mL lysozyme and DNase. The sample was centrifuged at 40,000 × g for 30 min. His_6-tagged HutZ was purified by affinity chromatography using a HisTrap HP column (GE Healthcare, Uppsala, Sweden). Eluted HutZ was collected and then applied to a gel-filtration column (HiLoad 16/60 Superdex 200 pg, GE Healthcare) equilibrated with 50 mM Tris-HCl, 150 mM NaCl (pH 8.0).

Mutagenesis was conducted utilizing a PrimeSTAR mutagenesis basal kit from TaKaRa Bio (Otsu, Japan). DNA oligonucleotides were purchased from Eurofins Genomics (Tokyo, Japan). The primers employed for the A31V mutant were 5'-CAA CTG GTG ACA GTC GAT GCG CAA GGT-3' (forward) and 5'-GAC TGT CAC CAG TTG CAG CGT TTT ACG-3' (reverse). The introduced mutation was verified by sequencing (Eurofins Genomics).

Spectroscopy

Optical spectra of purified proteins were recorded with a V-660 UV-vis spectrophotometer at 25 °C (Jasco, Tokyo, Japan). pH titration of heme-reconstituted HutZ in the ferric form was conducted by obtaining absorption spectra at different pH values, achieved by adding small amounts of 1 M HCl to the protein solution in 50 mM sodium phosphate or borate buffer; actual pH was measured using a micro pH electrode (Horiba, Kyoto, Japan). pK_a values were determined by fitting data for the fraction of the alkaline form as a function of pH to the Henderson-Hasselbalch equation.

Resonance Raman spectra were obtained using a single monochromator (SPEX500M, Jobin Yvon, NJ, USA) equipped with a liquid nitrogen-cooled CCD detector (Spec-10:400B/LN, Roper Scientific, Princeton, NJ, USA). The excitation wavelength employed was 413.1 nm, delivered by a krypton ion laser (BeamLok 2060, Spectra Physics, CA, USA). The laser power at the sample point was adjusted to 0.1 mW for the CO-bound form to prevent photodissociation. Raman shifts were calibrated with indene, CCl_4, acetone, and an aqueous solution of ferrocyanide. The accuracy of the peak positions of well-defined Raman bands was ±1 cm^{-1}. Sample concentration for Raman experiments was approximately 10 μM in 50 mM Tris-HCl and 150 mM NaCl (pH 8.0).

Fluorescence spectra were recorded using a FP-8500 fluorescence spectrometer (Jasco). The protein samples were excited at 295 nm to avoid any contribution from tyrosine residues. The HutZ concentration in samples was 10 μM in 50 mM Tris-HCl and 150 mM NaCl (pH 8.0). The distance (r) between tryptophan and heme was estimated from the efficiency (E) of Förster energy transfer from tryptophan to heme, defined as

$$E = \frac{R_0^6}{R_0^6 + r^6} \quad (1)$$

where R_0 is the Förster distance. We used R_0 of 29 A for heme and tryptophan.[48] The energy transfer efficiency, E, was calculated using the fluorescence intensity of apo-HutZ (F_{apo}) and heme-HutZ (F_{heme}), given by

$$E = \frac{F_{apo} - F_{heme}}{F_{apo}} \quad (2)$$

We assumed the dipole moments of heme and tryptophan do not changed.

Heme-Degradation Activity

The heme-degradation reaction of HutZ was monitored by spectrophotometry. Briefly, 1.9 mL of hemin-reconstituted protein solution (final concentration, 10 μM) in 50 mM Tris-HCl and 150 mM NaCl (pH 8.0) was placed in a cuvette, and the reaction was started by adding 100 μl of 2 mM H_2O_2 or 20 mM ascorbic acid in the same buffer at 25 °C. Spectra were recorded at 1-min intervals for 10 min for H_2O_2 (final

concentration, 0.1 mM), and 2-min intervals for 30 min for ascorbic acid (final concentration, 1 mM). In the case of reactions with ascorbic acid, 1 mg/mL of bovine liver catalase was added to suppress H_2O_2. After the reaction, ferrozine (Dojindo, Kumamoto, Japan) was added to a final concentration of 1 mM. The amount of released iron was calculated by measuring absorbance using an extinction coefficient at 562 nm (ε_{562}) of 29 $mM^{-1}cm^{-1}$. Degradation activity was determined by measuring the ratio of the concentration of ferrozine-captured iron to that of the applied protein.

Kinetic analyses of verdoheme formation were performed using a stopped-flow apparatus (Unisoku, Osaka, Japan). The reaction was monitored immediately after mixing equal volumes of 10 μM HutZ (50 mM MES and 150 mM NaCl (pH 6.0), or 50 mM Tris-HCl and 150 mM NaCl (pH 8.0)) and 200 μM H_2O_2. The absorbance decay was fitted using a single-exponential equation.

Redox Midpoint Potential and Heme Reduction Rate

The redox midpoint potential (E_m) for the Fe^{2+}/Fe^{3+} couple was determined by potentiometric titration under anaerobic conditions at 25 °C with continuous flow of humidified nitrogen gas. The three-electrode configuration used consisted of a platinum wire mesh as a working electrode, a platinum wire as a counter-electrode, and a saturated Ag/AgCl electrode as a reference electrode. The potentials of these electrodes were controlled by an HSV-110 potentiostat/galvanostat (Hokuto Denko, Tokyo, Japan). Test samples (0.5 mL) used contained 30 μM protein in 50 mM Tris-HCl and 150 mM NaCl (pH 8.0) or 50 mM MES and 150 mM NaCl (pH 6.0). The following redox mediators, at a final concentration of 1 μM each, were used to facilitate the equilibrium between the electrode and the reaction mixture: *N*,*N*,*N*',*N*'-tetramethyl-*p*-phenylenediamine (E_m = +260 mV), 2,6-dichlorophenolindophenol (E_m = +217 mV), 1,2-naphthoquinone (E_m = +145 mV), phenazine methosulfate (E_m = +80 mV), gallocyanine (E_m = +20 mV), indigo trisulfonate (E_m = –80 mV), 2-hydroxy-1, 4-naphthoquinone (E_m = –120 mV), anthraquinone-2-sulfonic acid sodium salt monohydrate (E_m = –230 mV), benzyl viologen (E_m = –350 mV), and methyl viologen (E_m = –440 mV). Absorption spectra were recorded from 350 to 700 nm using a Hitachi U-3310 UV-vis spectrophotometer equipped with a Peltier-type temperature-control system (Tokyo, Japan). The potential of the working electrode was decreased in 25 or 50 mV steps until the protein was fully reduced, and increased stepwise until reoxidation was complete. Heme reduction was monitored by measuring the increase in Soret absorption bands. Potential values are expressed relative to the normal standard hydrogen electrode (SHE) by adding 208 mV to the imposed potentials. Titration data were analyzed by fitting to the Nernst equation for a single-electron process. Data were collected in reductive and oxidative directions, and were reproducible within 10 mV.

The reduction rate of heme, k_{red}, was determined by following changes in absorbance at 418 nm.[31] A 5 μM ferric heme-HutZ complex was reduced by addition of 1 mM ascorbic acid. Although an oxygen scavenging system composed of glucose, glucose oxidase, and catalase was added to the solution to maintain anaerobiosis,[49] the reaction was conducted under a CO atmosphere to prevent re-oxidation or degradation of heme by contaminating O_2. The k_{red} value was obtained by fitting the time course of the changes in absorbance to a single-exponential expression.

3. Results

Heme-Degradation Activity of HutZ

In our previous study, we found that HutZ has an ability of heme degradation.[25] In the reaction of heme-HutZ with hydrogen peroxide (H_2O_2), absorption of the Soret band decreased and a new band appeared at 652 nm, which was assigned as ferric verdoheme. Further oxidation of verdoheme led to biliverdin formation (*m/z* 583.3), as identified by mass spectroscopy (Fig. S2†). We conducted the same experiment using myoglobin. In the case of myoglobin, absorption of the Soret band decreased, which was accompanied with a red-shift (408 → 421 nm) (Fig. S3A†). However, the decrease in the Soret absorption was not due to the formation of verdoheme, but the formation of the ferryl species (compound II), because the intensity of the Soret band regained and the maximum of the Soret band shifted to the original position after the addition of guaiacol (Fig. S3A†).

We previously observed the heme-degradation reaction under the single-turnover condition.[25,26,31,37] We here conducted the reaction in the presence of 2 equivalents of heme. When the reaction was initiated by the addition of HutZ to the solution containing 2 equivalent of heme, ascorbic acid and catalase, the heme-degradation ratio, defined as the ratio of iron concentration captured by ferrozine to the initial protein concentration, was ~160% (Fig. S3B†). A similar result was obtained when 1 equivalent of heme-bound HutZ was reacted in the presence of additional 1 equivalent of heme (Fig. S3C†). Considering that the heme-degradation ratio of HutZ was 86% under the single-turnover condition,[31] HutZ was likely to catalytically degrade heme. Consequently, we concluded

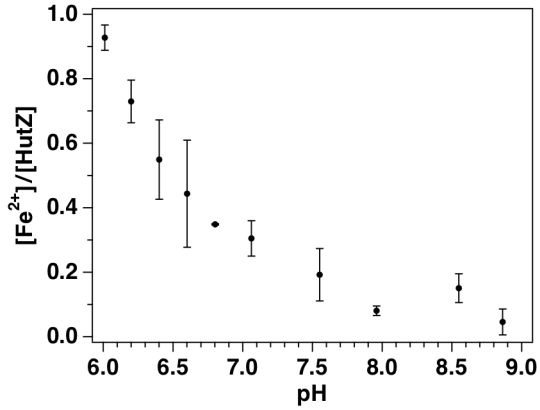

Fig. 2 pH dependence of the heme-degradation activity of heme-WT HutZ, determined by the amount of liberated iron.

that HutZ definitely has a heme-degradation ability.

One marked feature of the heme-degradation reaction by HutZ is its pH dependence.[25] Fig. 2 shows a plot of ascorbic acid-supported heme-degradation activity, defined as the ratio of the iron concentration captured by ferrozine to the initial heme concentration 60 min after the reaction, as a function of pH. This finding raised the possibility of a pH-dependent structural change around the heme-binding site. Indeed, UV-vis absorption spectra of heme-HutZ also exhibited pH dependence.[25] Absorption spectra of the ferric heme reflect the protonation (or deprotonation) of the axially ligated water molecule. The ferric heme complexed with HutZ at pH 6.0 is high spin (Fe^{3+}-H_2O), whereas that at pH 8.0 is low spin (Fe^{3+}-OH^-).[25] The pK_a value of the transition between high-spin and low-spin heme for heme-HutZ is less than 7.[25] We examined here the pH-dependent conformational change of HutZ using fluorescence spectroscopy. HutZ possesses a single tryptophan at position 109, which exists in a different subunit from that containing a heme axial ligand, His170 (Fig. 3).

The fluorescence of Trp109 was observed at around 330 nm when excited at 295 nm. The fluorescence for the heme-bound HutZ was much smaller than that of heme-unbound HutZ (Fig. 4), suggesting that the fluorescence of Trp109 was quenched by heme. Using the intensity of the fluorescence at 331 nm of HutZ and heme-HutZ, we calculated the energy transfer efficiency, *E*, to be approximately 90% (Equation 2). On the basis of this value of *E* and the Förster distance between heme and tryptophan of 29 Å,[50] we calculated the distance between heme and Trp109 at pH 8.0 to be 16.7 Å (Equation 1), which is comparable to that between the heme iron and Cα of the analogous residue, Asp183, in HugZ (21 Å), estimated using the crystal structure of HugZ.[22] The intensity at 331 nm for heme-WT HutZ at pH 6.0 was larger than that at pH 8.0 by approximately 30% (Fig. 4). Thus, the decrease in the quenching of tryptophan fluorescence by energy transfer to heme indicated that the distance between heme and Trp109 at pH 6.0 was greater than that at pH 8.0 by < 2 Å (Fig. S4†).

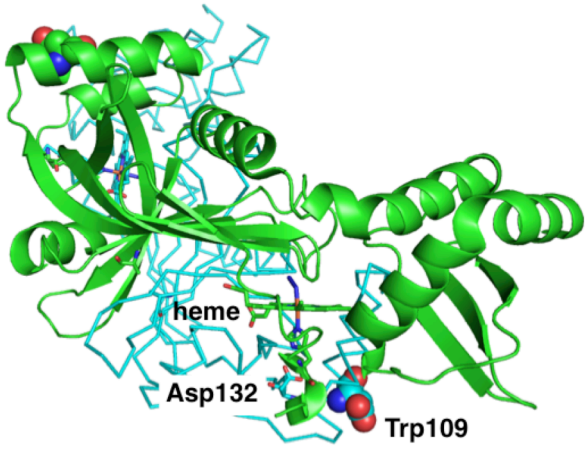

Fig. 3 Location of Trp109 and heme on the HugZ crystal structure (PBD 3GAS). Residues are numbered according to the amino acid sequence of HutZ from *V. cholerae*. Green and cyan show each protomer. Trp109 is present in a different protomer (green) from that (cyan) containing nearby Asp132.

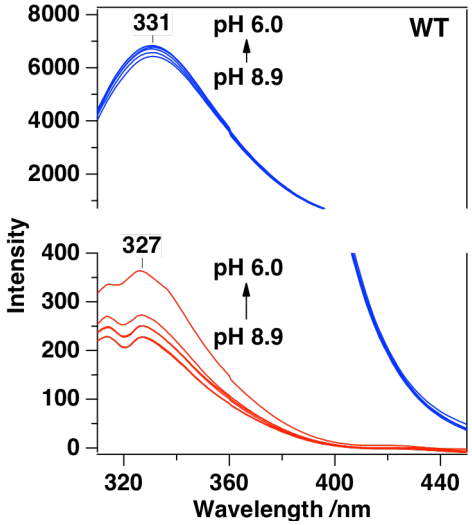

Fig. 4 Fluorescence energy transfer from Trp109 to heme. Fluorescence spectra of HutZ (blue) and heme-HutZ (red) at pH 6.0, 6.6, 7.1, 7.6, 8.1, and 8.9. The spectra were recorded with excitation at 295 nm. The sample concentration was 10 μM.

Reduction of Heme-HutZ

Since most of the heme remained in its ferric state during the ascorbate-dependent heme degradation at pH 8.0,[25] the rate-determining step of this reaction is likely the initial reduction of the ferric heme (Scheme 1). To test this, we compared the heme-reduction rates at pH 6.0 and 8.0. Fig. 5A shows time courses of absorption changes after the addition of ascorbic acid to ferric heme-HutZ in the presence of CO. Upon reduction, the Soret maximum at 412 nm underwent a red shift to 418 nm—the same position as the Soret peak in the CO-bound form.[25] Rapid CO binding to the ferrous heme prevents re-oxidation to ferric heme or undesirable heme degradation. The time course of absorbance changes at 418 nm at pH 6.0 was well fitted to a single-exponential function, yielding a ferric heme reduction rate, k_{red}, of 2.4 ± 0.1 h^{-1} at pH 6.0. Upon elevating the pH to 8.0, the reduction rate decreased by approximately 3-fold (0.86 ± 0.08 h^{-1}), consistent with the lower activity at the higher pH.

One of the factors that contributes to the slower reduction rate of heme-HutZ at pH 8.0 is strong electron donation from the proximal heme ligand, as evidenced by the fact that the correlation plot of $\nu_{Fe\text{-}CO}$ versus $\nu_{C\text{-}O}$ for heme-HutZ deviates from the line for proteins possessing neutral His as a heme ligand.[25] To confirm the extent of electron donation to the heme iron, we measured the reduction potential of the ferric heme. A plot of the relative ratio of ferrous heme against the measured potential is shown in Fig. 5B. For the reductive titration, a linear fit of the data obtained at 426 nm to the Nernst equation yielded the midpoint reduction potential for the Fe^{2+}/Fe^{3+} couple, E_m. The E_m potential at pH 8.0 was –176 ± 22 mV versus a standard hydrogen electrode (SHE), a value much lower than that reported for HO-1 (–65 mV).[51] Decreasing the pH of the protein solution to 6.0 increased the

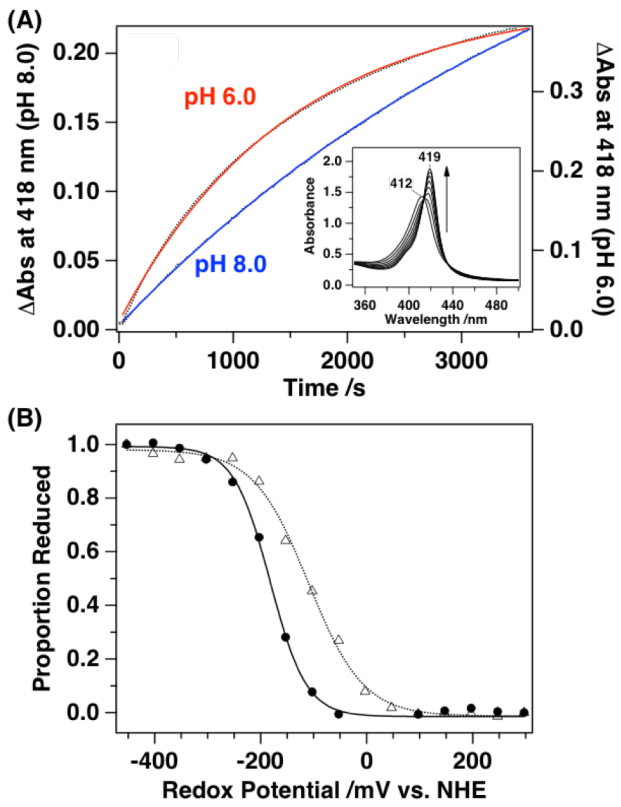

Fig. 5 Reduction of heme-HutZ. (A) Determination of the ferric heme reduction rate. Time course of absorbance changes at 419 nm at pH 6.0 (red line) and pH 8.0 (blue line) after the addition of ascorbic acid (final concentration, 1 mM) to ferric heme-HutZ under a CO atmosphere. Fitted curves are also shown in solid lines. The inset shows spectral changes of ferric heme-HutZ in the Soret region during reduction at pH 8.0. (B) Determination of the reduction potential (E_m) of heme. Redox titration curve for the heme-HutZ complex monitored by optical spectroscopy at 25 °C; (●) pH 8.0 and (△) pH 6.0. The ratio of reduced to oxidized heme was determined by changes in absorbance at 426 nm. The solid line represents a fit of experimental points to the Nernst equation. Reduction potentials are reported relative to SHE.

E_m potential to –142 ± 27 mV, consistent with easier heme reduction at lower pH.

Structural Characterization of the Heme-A31V Mutant

We postulated that the pH-dependent changes in the distance between heme and Trp109 is triggered by the spin state change in the heme distal site, which is transmitted to the proximal site and causes alternation of electron donation form the heme axial ligand. To confirm the relationship between the conformational change and the heme-degradation activity, we mutated an amino acid residue at the subunit-subunit interface. Although the crystal structure of heme-HutZ is not available, that of HugZ, a homologous protein from *H. pylori*, suggested that Ala31 in HutZ is located at the interface of two protomers (Fig. 1, Fig. S5†).[22] Thus, we introduced a bulky residue, Val, at position 31 (A31V) into the dimer interface, which was supposed to affect the conformational change connecting the distal and proximal heme sites.

The A31V mutant was purified using the same protocol as used for wild-type (WT) HutZ, and was isolated as an apoprotein. Gel filtration chromatography showed that the A31V mutant, like WT HutZ, existed as a dimer (Fig. S6†). The absorption spectrum of the ferric heme-A31V mutant at pH 8.0 resembled that of heme-WT HutZ (Fig. S7†), indicating that the spin state of heme at pH 8.0 was not altered by the mutation.

The degree of electron donation from the heme proximal ligand can be estimated from a correlation plot of $\nu_{Fe\text{-}CO}$ versus $\nu_{C\text{-}O}$ of the CO-bound heme.[52,53] The frequencies of $\nu_{Fe\text{-}CO}$ and $\nu_{C\text{-}O}$ of the heme-A31V mutant were 497 and 1959 cm^{-1}, respectively (Fig. 6A, B). The $\nu_{Fe\text{-}CO}$ of the heme-A31V mutant was downshifted by 8 cm^{-1} compared with that of heme-WT HutZ, whereas $\nu_{C\text{-}O}$ was upshifted by 24 cm^{-1}. Because of these frequency shifts, the correlation plot of $\nu_{Fe\text{-}CO}$ versus $\nu_{C\text{-}O}$ for the heme-A31V mutant fell on the line of proteins containing a neutral His as an axial ligand (Fig. 6C), suggesting that the mutation of Ala31 to Val decreased the imidazolate character of the proximal His. Electron donation from the proximal His was also estimated from the heme reduction rate. The k_{red} of the heme-A31V mutant at pH 8.0 was 2.3 ± 0.2 h^{-1} (Fig. S8†), which was almost the same as that of heme-WT HutZ at pH 6.0. This result also supports the conclusion that the proximal site of the heme-A31V mutant at pH 8.0 is close to that of heme-WT HutZ at pH 6.0, but not at pH 8.0.

pH-Dependent Conformational Change of the A31V Mutant.

To examine the changes in the distance between heme and Trp109 in the A31V mutant, we measured fluorescence spectra of tryptophan. The fluorescence intensity at 331 nm for the heme-A31V mutant was considerably larger than that for heme-WT HutZ (Figs. 3 and 7), which indicates that the Trp109–heme distance is much longer in the heme-A31V mutant than in heme-WT. Thus, the heme-A31V mutant also exhibited a pH-dependent change in conformation (Fig. 7). The distance between heme and Trp109 of the heme-A31V mutant was estimated to be 24–27 Å, which is much larger than that of heme-WT HutZ (Fig. S4†).

Introduction of Leu, a larger amino acid, at position 109 (A31L), also resulted in larger fluorescence intensity at 331 nm comparable to that of the heme-A31V mutant (Fig. S9A†). In contrast to the A31L mutant, substitution of Ala31 with Gly (A31G) did not affect the fluorescence intensity (Fig. S9B†). Because Trp109 is present in a different subunit from that containing the heme axial ligand His170, substitution of the larger side chain at Ala31 would cause distortion at the dimer interface, elongating the distance between heme and Trp109 (Fig. S4†).

The absorption spectrum of the heme-A31V mutant at pH 6.0 was indistinguishable from that at pH 8.0 (Fig. 8), indicating a shift in the pK_a of this mutant for the transition between high-spin and low-spin heme. To obtain the pK_a, we measured absorption spectra of the heme-A31V mutant in the pH range, 6.0–8.9. As shown in Fig. 8, absorption spectra of the heme-A31V mutant were almost independent of pH in this range, indicating that the pK_a was less than 6.

Heme-Degradation Activity of the Heme-A31V Mutant.

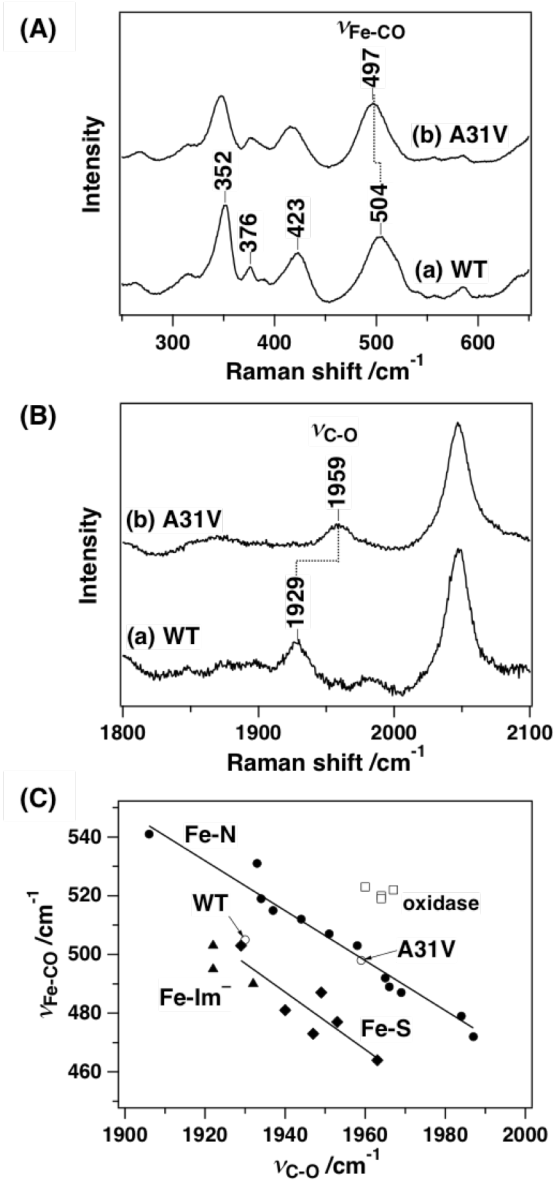

Fig. 6 Resonance Raman spectra of the heme-A31V mutant. Resonance Raman spectra of CO-bound state with excitation at 413.1 nm in low- (A) and high-frequency (B) regions. (C) Correlation between frequencies of ν_{Fe-CO} and ν_{C-O} stretching modes. The two solid lines correspond to correlations for proximal imidazoles (●), proximal imidazolates (▲), and thiolate-ligated hemoproteins (◆). Data points for oxidase superfamilies are depicted as solid open squares. The data point for HutZ is presented as an open circle. Data showing an inverse correlation between nFe-CO and nC-O are taken from previous reports. The protein concentration was 10 mM in 50 mM Tris-HCl, 150 mM NaCl (pH 8.0).

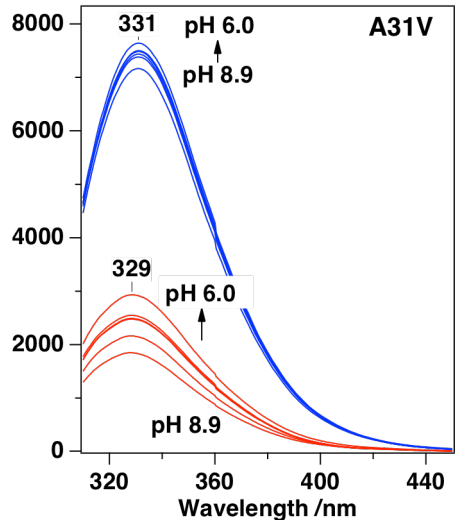

Fig. 7 Fluorescence energy transfer from Trp109 to heme. Fluorescence spectra of heme-A31V mutant HutZ (blue) and heme-HutZ (red) at pH 6.0, 6.6, 7.1, 7.6, 8.1, and 8.9. The spectra were recorded with excitation at 295 nm. The sample concentration was 10 μM.

The heme-degradation reaction of the heme-A31V mutant at pH 8.0 was investigated using ascorbic acid as an electron donor. Under these conditions, the Soret band gradually diminished, indicating that heme was degraded by ascorbic acid, even at pH 8.0 (Fig. 9A). To quantify the amount of iron released from the broken heme, we added ferrozine to the solution 30 min after initiation of the reaction. Despite the decreased Soret band, no band appeared at 562 nm (Fig. 9A), implying that iron was not released from the heme in the reaction of the heme-A31V mutant with ascorbic acid at pH 8.0. Because the WT HutZ is converted to the active form at pH 6.0, we performed the same reaction at pH 6.0. Again, iron was not released from the heme in the reaction of the heme-A31V mutant under these conditions (Fig. 9B). In spite of the larger heme reduction rate (Fig. 5A), elongated heme-Trp109 distance (Fig. 7, Fig. S4†), and less electron donation from the heme axial ligand (Figs. 5A, 6C), the A31V mutant did not show heme-degradation activity when ascorbic acid was used as electron source.

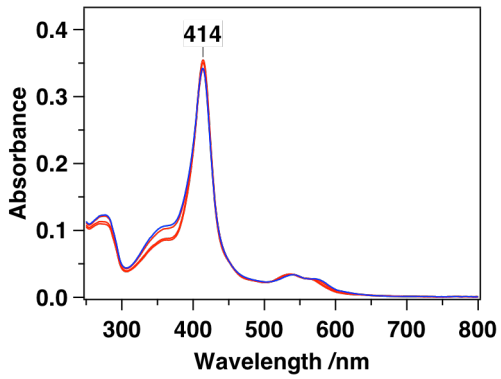

Fig. 8 pH dependence of the absorption spectra of the ferric heme-A31V mutant. Spectra were recorded at pH 5.5, 5.8, 6.0, 6.4, 6.9, 7.1, 7.4, 7.6, 8.1, 8.5, and 8.9. The spectrum at pH 8.9 is shown in blue.

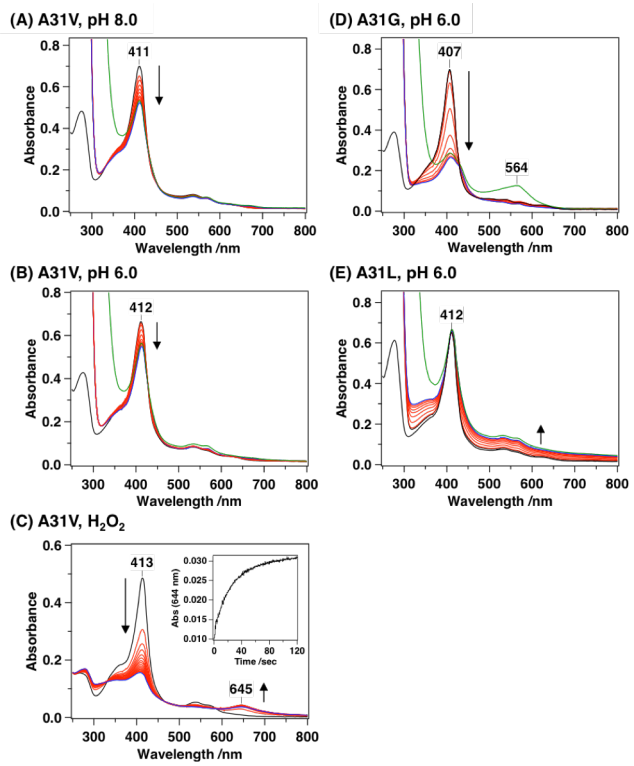

Fig. 9 Heme-degradation reaction of the heme-Ala31 mutants. Reaction of the heme-A31V mutant with ascorbic acid in the presence of catalase at (A) pH 8.0 and (B) pH 6.0. The green line showed the spectra after addition of ferrozine 30 min after initiation of the reaction. The final concentration of ascorbic acid was 1 mM. Spectra were measured before addition of ascorbic acid and at 4-min intervals for 30 min after addition of ascorbic acid. (C) Reaction of the heme-A31V mutant with H_2O_2 at pH 8.0. Spectra were measured before addition of H_2O_2 and at 1-min intervals for 10 min after the addition of H_2O_2. Inset: Time course of absorbance at 644 nm after the reaction with H_2O_2 at pH 8.0. Reaction of the heme-A31L (D) and A31G (E) mutants with ascorbic acid in the presence of catalase at pH 6.0. The reaction condition was the same as (B).

Next, to determine whether the mutation itself led to loss of the heme-degradation activity, we monitored the reaction of the heme-A31V mutant with H_2O_2 at pH 8.0. The Soret band diminished immediately after the addition of H_2O_2 with a concomitant increase in a band at 644 nm, indicating the formation of verdoheme, as was the case for heme-WT HutZ. Although the band at 644 nm, which is derived from verdoheme,[26] appeared, the absorbance at 644 nm in the reaction of the heme-A31V mutant with H_2O_2 was approximately 70% of that of heme-WT (Fig. 9C).[25] These results indicate that the A31V mutant is a slightly less efficient heme-degrading enzyme or verdoheme of the A31V mutant is somewhat unstable to degradation. However, the rate constant for the increase in the band at 644 nm for the heme-A31V mutant at pH 8.0 was 3.3×10^{-2} s^{-1} (Fig. 9C, inset), which was somewhat larger than that of the heme-WT HutZ (1.2×10^{-2} s^{-1}) (Fig. S8†). Therefore, the loss of ascorbic acid-assisted heme-degradation activity for the A31V mutant is likely due to that the mutation disrupted interactions between distal residue(s) and a network of water molecules that prevented protonation of the oxyferrous intermediate, similar to what was hypothesized for inhibition by iron chelators.[31]

The heme-degradation reaction of other two Ala31 mutants (A31G and A31L) was also examined. When the volume of the amino acid at position 31 was reduced by replacement of Ala31 with Gly, the ascorbic acid-dependent heme-degradation activity was retained as that of the WT HutZ (Fig. 9D). In contrast, when Leu was introduced, the mutant lost the activity, as observed for the A31V mutant (Fig. 9E).

Discussion

Role of Electron Donation from the Axial Heme Ligand to Heme in the Heme-Degradation Reaction by HutZ.

As reported in our previous study, heme-degradation activity of HutZ depends on pH.[25] The pH profile of the ascorbic acid-assisted heme-degradation was shown in Fig. 2. The conversion of heme-HutZ to a species with higher activity by decreasing the pH from 8.0 to 6.0 might be related to a change in the electrostatic character of the proximal His. At pH 6.0, the heme-HutZ reduction rate increased by about 3-fold (Fig. 5A), and the E_m value showed a positive shift by ~30 mV compared with that at pH 8.0 (Fig. 5B). These changes suggested a distinct decrease in electron donation from the proximal His at pH 6.0. The E_m value for heme peroxidases is negative (–120 to –320 mV),[54] and shows a dramatic positive shift following disruption of the proximal His-Asp hydrogen bond: –182 mV for WT cytochrome *c* peroxidase (C*c*P), –78 mV for the C*c*P D235A mutant, and –79 mV for the C*c*P D235N mutant.[32] In fact, the E_m value for heme-HutZ (–176 mV) is close to the values for heme peroxidases,[54] whereas that for heme-HO-1 (–65 mV)[51] is close to that of the C*c*P Asp mutants.[32] These results indicate that the proximal hydrogen bond in heme-HutZ at pH 8.0 is as strong as that in heme peroxidases,[32,55,56] whereas a moderate-strength hydrogen bond is involved in the heme-HO complex.[57,58] Rapid autoxidation of the oxyferrous heme of HutZ supports strong electron donation from the proximal ligand; the half-life ($t_{1/2}$) of the oxyferrous heme of HutZ at pH 8.0 is less than 10 s,[25] which is much faster than that observed for rat HO-1 ($t_{1/2} \approx 1.4$ h).[59]

As discussed above, the heme-degradation activity of HutZ was significantly enhanced at pH 6.0 (Fig. 2) with a concomitant increase in the heme-reduction rate (Fig. 5A). However, the increase in the heme reduction rate at pH 6.0 was only approximately 3-fold that at pH 8.0 (Fig. 5A). Therefore, heme was reduced by ascorbic acid even at pH 8.0, but heme degradation did not proceed under this condition. These results suggest that the process of heme reduction is not a major kinetic obstacle to heme degradation by HutZ at pH 8.0.

To confirm this, we constructed a series of substitution mutants of Ala31, which is located at the interface of the protomers and faces Ala31 on another protomer (Fig. 1). Mutating Ala31 to Val caused a decrease in electron donation from the proximal His at pH 8.0 to a level similar to that

observed in heme-WT HutZ at pH 6.0, judging from the reduction rate of heme (Fig. S8†), whereas the heme was retained in the low-spin state (Fig. S7†). Therefore, this mutant appeared to be suitable for estimating the contribution of proximal electron donation to heme-degradation activity. As expected, the absorption, and resonance Raman spectra of the A31V mutant suggested that the mutation induced no prominent structural changes in the heme vicinity (Figs. 6, 8), because the mutation site is far from the active site (Fig. 1). However, the heme-degrading activity was significantly decreased (Fig. 9). This result supports the idea that electron donation from the proximal His is not the only factor involved in repressing the heme-degrading reaction of HutZ at pH 8.0.

Role of Subunit-Subunit Interactions in the Heme-Degradation Reaction by HutZ.

Unexpectedly, the pK_a value for the transition between high-spin and low-spin heme for the A31V mutant could not be accurately determined because the absorption spectra showed almost no pH dependence in the range of pH 6–9 (Fig. 8). It is well known that the pK_a value for this transition is correlated with the pK_a value of the distal amino acid residue(s).[60] The pK_a value for this transition in myoglobin is 8.9,[61] whereas that of a mutant myoglobin in which the distal His is replaced with Val or Leu is greater than 10.[60] Thus, the pK_a value reflects the character of the amino acid residue that interacts with the iron-bound water molecule. However, Ala31 is located far from heme (~20 Å) and thus is unlikely to interact directly with the heme ligand (Fig. 1).

Introduction of Val at position 31 resulted in a significant increase in tryptophan fluorescence (Fig. 7). Because this fluorescence is quenched by heme, the intensity reflects the distance between heme and tryptophan. Thus, the increased fluorescence intensity of the heme-A31V mutant is indicative of elongation of the distance between heme and Trp109 (24–27 Å). The intensity of the fluorescence spectrum of Trp109 for heme-WT HutZ depended on the pH (Fig. 4), as observed in the absorption spectra. Because Trp109 is located in the heme proximal site (Fig. 1), the transition between high-spin (Fe^{3+}-H_2O) and low-spin heme (Fe^{3+}-OH^-) that occurs in the heme distal site also involves a structural change in the heme proximal site. The distance between heme and Trp109 in heme-WT HutZ was estimated to be 17–18 Å, which is smaller than that in the heme-A31V mutant (24–27 Å) (Fig. S4†). These results suggest that introduction of Val at position 31 extended the distance between heme and Trp109, and prevented the spin-state transition from low spin to high spin, leading to a loss of activity.

Replacement of Ala31 with Val caused heme-HutZ to adopt a chimeric state: low-spin heme with a weak proximal hydrogen bond (Fig. 8). In the reaction of the heme-A31V mutant with ascorbic acid, almost no iron was released (Fig. 9A, B). Therefore, diminished electron donation from the proximal ligand of the heme-A31V mutant did not lead to enhanced HutZ activity. Although the heme-A31V mutant was insensitive to ascorbic acid (Fig. 9A, B), it was active towards H_2O_2 (Fig. 9C), indicating that the mutant retained heme-degradation activity. Like the heme-A31V mutant, the heme-A31L mutant also showed diminished heme-degradation activity (Fig. 9E), whereas the heme-A31G mutant showed the same level of activity as WT HutZ (Fig. 9D), and the fluorescence spectrum of the heme-A31G mutant was indistinguishable from that of WT HutZ (Figs. S4†, S9B†). These results indicate that communication between protomers via Ala31 is essential for the heme-degradation activity of HutZ. The high degree of conservation of Ala31 supports the importance of this interaction in the HugZ family (Fig. S6†).

Inactivation of heme-HutZ, in spite of the fact the heme is in the high-spin state, was also observed when the reaction was conducted in the presence of iron chelators, such as deferoxamine or ferrozine.[31] Heme-HutZ in the presence of ferrozine was inactive to ascorbic acid, even at pH 6.0, although verdoheme was formed in the reaction with H_2O_2. In this case, we propose that the chelators perturb proton transfer from water molecules to the reduced oxyferrous intermediate, Fe^{3+}-OO^-.[31] Thus, a possible explanation for the lower activity of the A31V mutant is that the mutation places distal amino acid residues in an inappropriate position by disrupting the linkage between protomers, thereby causing a perturbation of the water cluster that renders it unsuitable for heme degradation.

On the basis of our findings, we propose a possible scenario to account for HutZ activation (Fig. 10). According to this model, protonation of the low-spin heme (Fe^{3+}-OH^-) to the

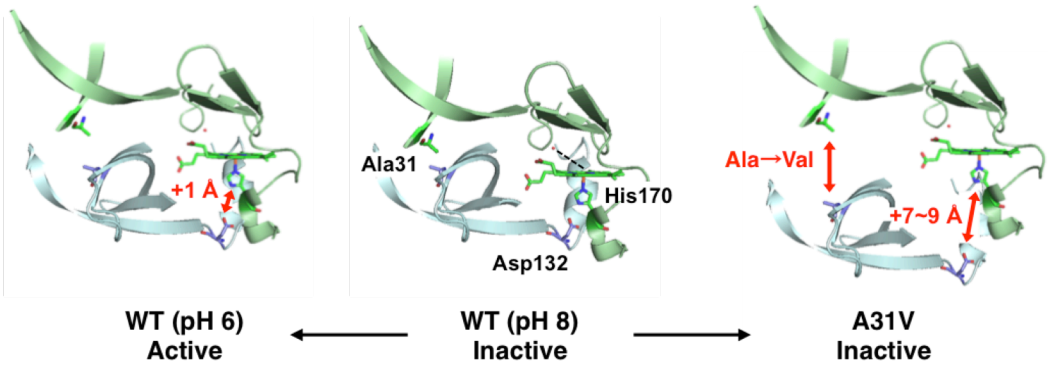

Fig. 10 Proposed regulation mechanism of heme degradation by HutZ.

high-spin heme (Fe^{3+}-H_2O) induces reorganization of the water cluster, facilitating its function as a proton source. These structural changes in the heme distal site are transmitted to the proximal site through subunit-subunit interactions and modulate the strength of the hydrogen bond between Asp132 and His170, leading to a reduction in electron donation from the proximal His to heme. Because of these changes, heme is susceptible to reduction, and autooxidation of oxyferrous heme is repressed, leading to heme degradation. Thus, intersubunit communication between the heme distal and proximal sites through subunit-subunit interactions is essential for HutZ to degrade heme.

As discussed above, we propose that the subunit-subunit interactions are essential for the heme-degradation reaction by HutZ. To modulate the strength of the interactions, HutZ likely requires some effector molecule(s) or protein(s). One possibility is that effector molecule(s) enhance the expression of Hut proteins. We recently found that HutX, which is expressed as part of the *hutWXZ* operon, is a heme transfer protein for HutZ.[62] However, HutX does not enhance the activity of HutZ. Another possibility is a reductase protein. The degradation of heme by HutZ requires electrons, which could be supplied by reductase. The interaction of HutZ with reductase could cause a conformational change in HutZ that modulates the strength of the His-Asp hydrogen bond, leading to an increase in the redox potential of the heme and rapid heme degradation. Although HutW is homologous protein of ChuW, which is recently proposed an anaerobic heme-degrading enzyme,[21] it is also a possible reductase of HutZ because of the presence of the putative Fe-S cluster. Unfortunately, we failed to express it in *E. coli*. Finding such regulatory molecules will provide a means for bacteria to fine-tune their expression of heme-degrading activity in order to rapidly adjust to changes in nutrient levels.

Conclusions

In summary, decreasing the pH from 8.0 to 6.0 converted HutZ to the active form by virtue of a slight structural change at the heme distal site accompanied by spin-state conversion from low spin to high spin. This conformational change would modulate the imidazolate character of the proximal His, and thus the propensity for heme reduction as well as autooxidation of the oxyferrous heme. The mutation of Ala31, which is located at the dimer interface, to Val or Leu resulted in diminished electron donation from the proximal His, but did not result in enhanced activity. These results indicate that strong electron donation is not the only factor that determines the activity of HutZ. Instead, the subunit-subunit interactions, which transmit structural changes at the heme distal site to the proximal site, appear to be essential for the heme-degradation activity. Because HutZ, unlike human HOs, is a dimeric protein,[25] such an inactive-to-active switch for the heme-degrading reaction with a conformational change at the dimer interface is a prominent feature of HutZ, and would be important for intracellular iron homeostasis in *V. cholerae*.

Conflicts of interest

There are no conflicts to declare".

Acknowledgements

The authors wish to acknowledge Dr. Toshitaka Matsui for measurement of the mass spectrometry. This study was supported in part by Grants-in-Aid for Scientific Research (16K05835 to T.U., and 15H00909 to K.I.) from the Ministry of Culture, Education, Sports, Science, and Technology (MEXT) of Japan.

Notes and references

1 L. L. Anzaldi and E. P. Skaar, *Infect. Immun.*, 2010, **78**, 4977–4989.
2 C. A. Genco and D. W. Dixon, *Mol. Microbiol.*, 2001, **39**, 1–11.
3 U. A. Ochsner, Z. Johnson and M. L. Vasil, *Microbiology*, 2000, **146**, 185–198.
4 J. A. Stoebner and S. M. Payne, *Infect. Immun.*, 1988, **56**, 2891–2895.
5 C. Wandersman and I. Stojiljkovic, *Curr. Opin. Microbiol.*, 2000, **3**, 215–220.
6 A. Wilks and K. A. Burkhard, *Nat. Prod. Rep.*, 2007, **24**, 511–522.
7 P. R. Ortiz de Montellano, *Acc. Chem. Res.*, 1998, **31**, 543–549.
8 G. Kikuchi, T. Yoshida and M. Noguchi, *Biochem. Biophys. Res. Commun.*, 2005, **338**, 558–567.
9 T. Matsui, M. Unno and M. Ikeda-Saito, *Acc. Chem. Res.*, 2010, **43**, 240–247.
10 A. Wilks and M. P. Schmitt, *J. Biol. Chem.*, 1998, **273**, 837–841.
11 W. Zhu and A. Wilks, *J. Bacteriol.*, 2000, **182**, 6783–6790.
12 D. J. Schuller, W. M. Zhu, I. Stojiljkovic, A. Wilks and T. L. Poulos, *Biochemistry*, 2001, **40**, 11552–11558.
13 M. Ratliff, W. Zhu, R. Deshmukh, A. Wilks and I. Stojiljkovic, *J. Bacteriol.*, 2001, **183**, 6394–6403.
14 M. L. Pendrak, M. P. Chao, S. S. Yan and D. D. Roberts, *J. Biol. Chem.*, 2004, **279**, 3426–3433.
15 E. P. Skaar, A. H. Gaspar and O. Schneewind, *J. Biol. Chem.*, 2004, **279**, 436–443.
16 E. P. Skaar, A. H. Gaspar and O. Schneewind, *J. Bacteriol.*, 2006, **188**, 1071–1080.
17 R. Wu, E. P. Skaar, R. Zhang, G. Joachimiak, P. Gornicki, O. Schneewind and A. Joachimiak, *J. Biol. Chem.*, 2005, **280**, 2840–2846.
18 T. Matsui, S. Nambu, Y. Ono, C. W. Goulding, K. Tsumoto and M. Ikeda-Saito, *Biochemistry*, 2013, **52**, 3025–3027.
19 M. L. Reniere, G. N. Ukpabi, S. R. Harry, D. F. Stec, R. Krull, D. W. Wright, B. O. Bachmann, M. E. Murphy and E. P. Skaar, *Mol. Microbiol.*, 2010, **75**, 1529–1538.
20 T. Matsui, S. Nambu, C. W. Goulding, S. Takahashi, H. Fujii and M. Ikeda-Saito, *Proc. Natl. Acad. Sci. U. S. A.*, 2016, **113**, 3779–3784.

21 J. W. LaMattina, D. B. Nix and W. N. Lanzilotta, *Proc. Natl. Acad. Sci.*, 2016, **113**, 12138–12143.

22 Y. Hu, F. Jiang, Y. Guo, X. Shen, Y. Zhang, R. Zhang, G. Guo, X. Mao, Q. Zou and D.-C. Wang, *J. Biol. Chem.*, 2011, **286**, 1537–1544.

23 Y. Guo, G. Guo, X. Mao, W. Zhang, J. Xiao, W. Tong, T. Liu, B. Xiao, X. Liu, Y. Feng and Q. Zou, *BMC Microbiol.*, 2008, **8**, 226.

24 J. F. Heidelberg, J. A. Eisen, W. C. Nelson, R. a Clayton, M. L. Gwinn, R. J. Dodson, D. H. Haft, E. K. Hickey, J. D. Peterson, L. Umayam, S. R. Gill, K. E. Nelson, T. D. Read, H. Tettelin, D. Richardson, M. D. Ermolaeva, J. Vamathevan, S. Bass, H. Qin, I. Dragoi, P. Sellers, L. McDonald, T. Utterback, R. D. Fleishmann, W. C. Nierman, O. White, S. L. Salzberg, H. O. Smith, R. R. Colwell, J. J. Mekalanos, J. C. Venter and C. M. Fraser, *Nature*, 2000, **406**, 477–483.

25 T. Uchida, Y. Sekine, T. Matsui, M. Ikeda-Saito and K. Ishimori, *Chem. Commun.*, 2012, **48**, 6741–6743.

26 T. Uchida, Y. Sekine, N. Dojun, A. Lewis-Ballester, I. Ishigami, T. Matsui, S.-R. Yeh and K. Ishimori, *Dalton Trans.*, 2017, **46**, 8104–8109.

27 J. Docherty, B. Masters, G. Firneisz and B. Schacter, *Biochem Biophys Res Commun.*, 1982, **105**, 1005–1013.

28 M. Noguchi, T. Yoshida and G. Kikuchi, *J. Biochem.*, 1982, **91**, 1479–1483.

29 T. Yoshinaga, S. Sassa and A. Kappas, *J. Biol. Chem.*, 1982, **257**, 7794–7802.

30 E. E. Wyckoff, M. Schmitt, A. Wilks and S. M. Payne, *J. Bacteriol.*, 2004, **186**, 4142–4151.

31 N. Dojun, Y. Sekine, K. Ishimori and T. Uchida, *Dalton Trans.*, 2017, **46**, 5147–5150.

32 D. B. Goodin and D. E. McRee, *Biochemistry*, 1993, **32**, 3313–3324.

33 B. C. Finzel, T. L. Poulos and J. Kraut, *J. Biol. Chem.*, 1984, **259**, 13027–13036.

34 T. L. Poulos, *J. Biol. Inorg. Chem.*, 1996, **1**, 356–359.

35 M. Sono, M. P. Roach, E. D. Coulter and J. H. Dawson, *Chem. Rev.*, 1996, **96**, 2841–2888.

36 A. Wilks and P. R. Ortiz de Montellano, *J. Biol. Chem.*, 1993, **268**, 22357–22362.

37 T. Uchida, N. Dojun, Y. Sekine and K. Ishimori, *Biochemistry*, 2017, **56**, 2723–2734.

38 S. Hu, A. J. Schneider and J. R. Kincaid, *J. Am. Chem. Soc.*, 1991, **113**, 4815–4822.

39 J. Lang, J. Santolini and M. Couture, *Biochemistry*, 2011, **50**, 10069–10081.

40 W. T. Potter, M. P. Tucker, R. A. Houtchens and W. S. Caughey, *Biochemistry*, 1987, **26**, 4699–4707.

41 S. Hirota, T. Ogura and T. Kitagawa, *J. Am. Chem. Soc.*, 1995, **117**, 821–822.

42 S. Takahashi, K. Ishikawa, N. Takeuchi, M. Ikeda-Saito, T. Yoshida and D. L. Rousseau, *J. Am. Chem. Soc.*, 1995, **117**, 6002–6006.

43 R. Deshmukh, Y. H. Zeng, L. M. Furci, H. W. Huang, B. N. Morgan, S. Sander, A. Y. Alontaga, R. A. Bunce, P. Moenne-Loccoz, M. Rivera and A. Wilks, *Biochemistry*, 2005, **44**, 13713–13723.

44 Y. H. Zeng, R. Deshmukh, G. A. Caignan, R. A. Bunce, M. Rivera and A. Wilks, *Biochemistry*, 2004, **43**, 5222–5238.

45 G. C. Chu, T. Tomita, F. D. Sönnichsen, T. Yoshida and M. Ikeda-Saito, *J. Biol. Chem.*, 1999, **274**, 24490–24496.

46 G. A. Caignan, R. Deshmukh, Y. H. Zeng, A. Wilks, R. A. Bunce and M. Rivera, *J. Am. Chem. Soc.*, 2003, **125**, 11842–11852.

47 T. Uchida, M. Sasaki, Y. Tanaka and K. Ishimori, *Biochemistry*, 2015, **54**, 6610–6621.

48 J. R. Lakowicz, *Principles of fluorescence spectroscopy*, Springer, New York, 3rd edn., 2006.

49 S. W. Englander, D. B. Calhoun and J. J. Englander, *Anal. Biochem.*, 1987, **161**, 300–306.

50 P. Wu and L. Brand, *Anal. Biochem.*, 1994, **218**, 1–13.

51 Y. Liu, P. Moënne-Loccoz, D. P. Hildebrand, A. Wilks, T. M. Loehr, A. G. Mauk and P. R. Ortiz de Montellano, *Biochemistry*, 1999, **38**, 3733–3743.

52 G. B. Ray, X. Y. Li, J. A. Ibers, J. L. Sessler and T. G. Spiro, *J. Am. Chem. Soc.*, 1994, **116**, 162–176.

53 N.-T. Yu and E. A. Kerr, in *Biological Applications of Raman Spectroscopy*, ed. T. G. Spiro, John Wiley & Sons, New York, III., 1988, pp. 97–131.

54 H. A. Harbury, *J. Biol. Chem.*, 1957, **225**, 1009–1024.

55 S. Hashimoto, J. Teraoka, T. Inubushi, T. Yonetani and T. Kitagawa, *J. Biol. Chem.*, 1986, **261**, 11110–11118.

56 G. Smulevich, J. M. Mauro, L. A. Fishel, A. M. English, J. Kraut and T. G. Spiro, *Biochemistry*, 1988, **27**, 5477–5485.

57 J. Sun, A. Wilks, P. R. Ortiz de Montellano and T. M. Loehr, *Biochemistry*, 1993, **32**, 14151–14157.

58 S. Takahashi, J. Wang, D. L. Rousseau, K. Ishikawa, T. Yoshida, J. R. Host and M. Ikeda-Saito, *J. Biol. Chem.*, 1994, **269**, 1010–1014.

59 H. Fujii, X. Zhang, T. Tomita, M. Ikeda-Saito and T. Yoshida, *J. Am. Chem. Soc.*, 2001, **123**, 6475–6484.

60 M. Ikeda-Saito, H. Hori, L. A. Andersson, R. C. Prince, I. J. Pickering, G. N. George, C. R. Sanders, R. S. Lutz, E. J. McKelvey and R. Mattera, *J. Biol. Chem.*, 1992, **267**, 22843–22852.

61 E. Antonini and M. Brunori, *Hemoglobin and myoglobin in their reactions with ligands*, Elsevier/North-Holland Biomedical Press, Amsterdam, 1971.

62 Y. Sekine, T. Tanzawa, Y. Tanaka, K. Ishimori and T. Uchida, *Biochemistry*, 2016, **55**, 884–893.